Gene Expression Profiling in the Striatum of *Per2* KO Mice Exhibiting More Vulnerable Responses against Methamphetamine

Mikyung Kim[1,2,†], Se Jin Jeon[3,†], Raly James Custodio[1], Hyun Jun Lee[1], Leandro Val Sayson[1], Darlene Mae D. Ortiz[1], Jae Hoon Cheong[4,*] and Hee Jin Kim[1,*]

[1]*Uimyung Research Institute for Neuroscience, Department of Pharmacy, Sahmyook University, Seoul 01795,*
[2]*Department of Chemistry Life Science, Sahmyook University, Seoul 01795,*
[3]*School of Medicine and Center for Neuroscience Research, Konkuk University, Seoul 05029,*
[4]*School of Pharmacy, Jeonbuk National University, Jeonju 54896, Republic of Korea*

Abstract

Drug addiction influences most communities directly or indirectly. Increasing studies have reported the relationship between circadian-related genes and drug addiction. *Per2* disrupted mice exhibited more vulnerable behavioral responses against some drugs including methamphetamine (METH). However, its roles and mechanisms are still not clear. Transcriptional profiling analysis in *Per2* knockout (KO) mice may provide a valuable tool to identify potential genetic involvement and pathways in enhanced behavioral responses against drugs. To explore the potential genetic involvement, we examined common differentially expressed genes (DEGs) in the striatum of drug naïve *Per2* KO/wild-type (WT) mice, and before/after METH treatment in *Per2* KO mice, but not in WT mice. We selected 9 common DEGs (*Ncald*, *Cpa6*, *Pklr*, *Ttc29*, *Cbr2*, *Egr2*, *Prg4*, *Lcn2*, and *Camsap2*) based on literature research. Among the common DEGs, *Ncald*, *Cpa6*, *Pklr*, and *Ttc29* showed higher expression levels in drug naïve *Per2* KO mice than in WT mice, while they were downregulated in *Per2* KO mice after METH treatment. In contrast, *Cbr2*, *Egr2*, *Prg4*, *Lcn2*, and *Camsap2* exhibited lower expression levels in drug naïve *Per2* KO mice than in WT mice, while they were upregulated after METH treatment in *Per2* KO mice. qRT-PCR analyses validated the expression patterns of 9 target genes before/after METH treatment in *Per2* KO and WT mice. Although further research is required to deeply understand the relationship and roles of the 9 target genes in drug addiction, the findings from the present study indicate that the target genes might play important roles in drug addiction.

Key Words: Addiction, Methamphetamine, *Per2*, Gene expression

INTRODUCTION

Drug addiction is a chronic relapsing brain disease, affecting most communities directly or indirectly. Many researches and institutions have tried to identify its causes and prevent its adverse consequences, and a few drug addiction targets have been identified (Nestler and Malenka, 2004; Everitt and Robbins, 2016). Dopaminergic projections are known to be associated with the processes of drug abuse and addiction (Volkow *et al*., 2017; Solinas *et al*., 2019), and dopaminergic neurons projecting from the ventral tegmental area (VTA) release dopamine neurotransmitters to the nucleus accumbens (NAc) and the prefrontal cortex (PFC), forming mesolimbic and mesocortical pathways, respectively. In addition to the dopaminergic system, a complex interaction between exogenous (i.e., environment) and endogenous (i.e., genes and circadian rhythms) factors is also known to cause drug addiction (Abarca *et al*., 2002; Kim *et al*., 2018). Recently, increasing studies have reported the relationship between disturbed circadian rhythms and drug addiction (Abarca *et al*., 2002; Kovanen *et al*., 2010; Hasler *et al*., 2012). Disturbed circadian rhythms lead to increased substance use such as alcohol and cocaine indicating that circadian rhythms might play important roles in drug addiction.

Per2 is one of the key genes that generates circadian rhythms (Albrecht *et al*., 2001). Virtually, its mutations in mice induce different responses to drugs. For instance, mice with *Per2* disruption consumed more alcohol and demonstrated

increased reward effects to cocaine, morphine, or methamphetamine (METH) (Abarca *et al*., 2002; Spanagel *et al*., 2005; Perreau-Lenz *et al*., 2010; Kim *et al*., 2019). In our previous study, *Per2* knockout (KO) mice (*Per2*^{tm1Drw}) displayed increased METH-induced locomotor sensitization and reward responses (Kim *et al*., 2019). Additionally, the expression levels of dopamine-related genes and dopamine changed in the striatum depending on the expression of *Per2*. These findings suggest that *Per2* might be one of the key genes to modulate drug addiction pathways, although mechanism of *Per2* function is still not clear. Thus, further studies should focus on the mechanisms of *Per2* in drug addiction.

Gene expression profiling might provide an ideal platform to elucidate the possible mechanisms of *Per2* in drug addiction. The goal of this study was to further understand the role of *Per2* in drug addiction using microarray analyses. In our previous study, we reported that METH-induced behavioral responses and dopamine levels in the striatum changed based on *Per2* expression (Kim *et al*., 2019). The striatum is the brain region associated with METH addiction responses in rodents and human, and is known to increase dopamine release following psychostimulants administrations (Chang *et al*., 2007; Caprioli *et al*., 2017; Kim *et al*., 2019). Therefore, we analyzed the differentially expressed genes (DEGs) in the striatum of *Per2* KO and wild-type (WT) mice, which showed different behavioral and molecular responses against METH.

MATERIALS AND METHODS

Drugs and materials

METH hydrochloride, purchased from Sigma-Aldrich Co (St. Louis, Mo, USA), was dissolved in physiological saline (0.9% w/v of NaCl), at a dose of 0.5 mg/kg intraperitoneally, as used in our previous study (Kim *et al*., 2019). TRIzol reagent was purchased from Invitrogen (Carlsbad, CA, USA), and the Hybrid-R™ kit was purchased from Geneall Biotechnology (Seoul, Korea). The AccuPower® CycleScript RT PreMix used to generate cDNA was obtained from Bioneer (Seoul, Korea). All primers for quantitative real-time PCR (qRT-PCR) were obtained from Cosmogenetech Co (Seoul, Korea), using a set of custom sequence-specific primers. SYBR® Green used to run qRT-PCR was purchased from SolGent Co (Daejeon, Korea).

Animals

Eight- to twelve-week-old male *Per2*^{tm1Drw} (–/–), and C57BL/6 mice were used in this study. The heterozygous *Per2*^{tm1Drw} (+/–) mutant mice (Bae *et al*., 2001) were obtained from the Jackson laboratory (Stock No.010492; JAX MICE®, ME, USA), and *Per2*^{tm1Drw} (–/–, KO) mice were derived by intercrossing heterozygous *Per2*^{tm1Drw} (+/–) and C57BL/6 mice, followed by crossing homozygous *Per2*^{tm1Drw} (–/–) mutant mice. The C57BL/6 mice were used as the control group because *Per2* KO were derived from C57BL/6 mice, which were obtained from Hanlim Laboratory Animals Co (Hwaseong, Korea). Each transgenic (TG) and WT mouse group was housed in an animal room under controlled conditions (12 h/12 h light/dark cycle, 7 AM-7 PM, and 22 ± 2°C) and fed *ad libitum*. All animal treatment and maintenance were performed in accordance with the Principles of Laboratory Animal Care (NIH Publication No. 85-23 revised 1985), and the Animal Care and Use Guidelines of Sahmyook Uni-

versity, Seoul, Korea (SYUIACUC2018-004).

Experiment time

METH treatment and collection of brain tissue samples were conducted at ZT 4-5, wherein ZT 0 indicates lights on (e.g., 7 AM) and ZT 12 indicates lights off (e.g., 7 PM), as previously described (Abarca *et al*., 2002; Hood *et al*., 2010; Kim *et al*., 2019). ZT 4-5 was selected based on previous reports (Abarca *et al*., 2002; Hood *et al*., 2010; Kim *et al*., 2019).

mRNA-Seq Data Analyses (Microarray)

Drug naïve animals and animals treated with METH for 7 days (*n*=3/group) were sacrificed by decapitation at ZT 4-5, and the extracted brain samples were separated into the target area, striatum, using the mouse brain matrix, and stored at –80°C. Total RNA was isolated, purified, and checked for quality. Total RNA was used to construct cDNA libraries with the TruSeq Stranded mRNA LT Sample Prep Kit (Illumina, San Diego, CA, USA). The protocol involved polyA-selected RNA extraction, RNA fragmentation, random hexamer primed reverse transcription and 100nt paired-end sequencing by Illumina NovaSeq 6000 (Illumina). The libraries were quantified using qPCR according to the qPCR Quantification Protocol Guide and qualified using an Agilent Technologies 2100 Bioanalyzer (Agilent, Santa Clara, CA, USA).

The raw reads from the sequencer were preprocessed to remove low quality and adapter sequences before analysis and aligned the processed reads to the *Mus musculus* (*mm10*) using HISAT v2.1.0 (The HISAT-genotype source code is available in a public GitHub repository). HISAT utilizes two types of indexes for alignment (a global, whole-genome index and tens of thousands of small local indexes). These indexes are constructed using the same BWT (Burrows–Wheeler transform)/ graph FM index (GFM) as Bowtie2 (Johns Hopkins University, MD, USA). Owing to its use of these efficient data structures and algorithms, HISAT generates spliced alignments several times faster than Bowtie and BWA. The reference genome sequence of *Mus musculus* (*mm10*) and annotation data were downloaded from the NCBI (https://www.ncbi.nlm.nih.gov/ genome/). The transcript assembly of known transcripts was then processed using StringTie v1.3.4d (Johns Hopkins University, MD, USA). Base on the results obtained, the expression abundance of the transcript and gene were calculated as read count or FPKM value (fragments per kilobase of exon per million fragments mapped) per sample. The expression profiles were used to perform additional analysis such as those of DEGs. In groups with different conditions, DEGs or transcripts can be filtered through statistical hypothesis testing.

Validation of microarray data by quantitative real-time PCR (qRT-PCR)

Drug naïve animals and animals treated with METH for 7 days (n=6-8/group) were sacrificed at ZT 4-5, and each brain sample was kept at –80°C immediately after extraction. Total RNA from the striatum was isolated and purified using TRIzol reagent and the Hybrid-R™ kit. The AccuPower® CycleScript RT PreMix was used to prepare cDNA, and all procedures were conducted in compliance with the manufacturer's instructions. Table 1 shows the sequences of each target gene's primer. A total volume of 20 µL (SYBR® Green 10 µL+forward primer 1 µL+reverse primer 1 µL+cDNA 2 µL+distilled water 6 µL) was used to run qRT-PCR. A housekeeping gene (GAP-

Table 1. Selected 9 genes primers for Real-time PCR

|	Forward (5`→3`)	Reverse (5`→3`)
Ncald	AGC ATG GAC AGA CTT CGT GG	CAG GAC TGG ATG GGT TTC CC
Cpa6	GTC TGG ATA GAC TGC GGC ATT	GTC TCT TGA CCG GGT CTT TC
Pklr	TAG GAG CAC CAG CAT CAT TG	CAT CCC TGC CTT GAT CAT CT
Ttc29	CTT CCC ATG ACT CAT ACA AGG C	CCC TTT GAA ATT CTG TTC CAG GT
Cbr2	GGG CAG GGA AAG GGA TTG G	CCA CAC ACA CGG GCT CTA TTC
Egr2	GCC AAG GCC GTA GAC AAA ATC	CCA CTC CGT TCA TCT GGT CA
Prg4	CGC CTT TTC CAA AGA TCA ATA CTA	GTG GTA ATT GCT CTT GCT GTT
Lcn2	ATG TAT GGC CGG TAC ACT CAG	AAC AAA TGC GAC ATC TGG CAC
Camsap2	CGA CCT CAG GCG GCT AAA	GAG GGC CTT TGA TCG GTG T
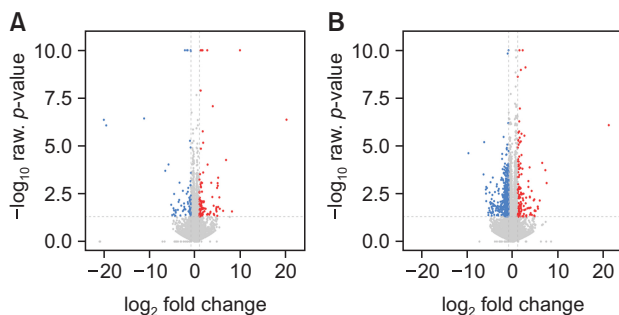
Fig. 1. Hierarchical clustering analysis of DEGs. Volcano plot showing the transcriptional changes in the striatum of drug naïve *Per2* KO/WT mice (A), and before/after METH treatments in *Per2* KO mice (B). Each circle represents one gene. The log fold change (FC) in the indicated genotype versus wild type is represented on the x-axis. The y-axis shows the log10 of the *p* value. A *p* value of 0.05 and a FC of 2 are indicated by grey lines. In the plot, the area above the genes is colored if they pass the thresholds for FDR and Log FC, red if they are upregulated and blue if they are downregulated.

DH) was used to normalize each value. All data were analyzed using the ΔΔCt method (Ct is defined as the threshold cycle).

Statistical analysis of gene expression level

The relative abundances of gene were measured in read count using StringTie. We performed statistical analysis to find DEGs using the estimates of abundances for each gene in the samples. Genes with more than one 'zero' read count values in the samples were excluded. Filtered data were log2-transformed and subjected to RLE normalization. Statistical significance of the differential expression data was determined using the nbinomWaldTest using DESeq2 and fold change (FC); the null hypothesis was that no difference exists among groups. False discovery rate (FDR) was controlled by adjusting the *p* value using the Benjamini-Hochberg algorithm. For the DEG set, hierarchical clustering analysis was performed using complete linkage and Euclidean distance as a measure of similarity. Gene-enrichment and Kyoto Encyclopedia of Genes and Genomes (KEGG) pathway analyses for all DEGs were also performed based on Gene Ontology (http://geneontology.org/), and KEGG pathway (https://www.genome.jp/kegg/) database, respectively. We performed functional analysis using STRING database online (https://string-db.org/) which aims to collect, score, and integrate all publicly available sources of

protein-protein interaction (PPI) information, and to complement these with computational predictions.

All qRT-PCR data are expressed as mean ± SEM and analyzed using two-way analysis of variance (ANOVA). When significant group differences were observed, the Bonferroni post-hoc tests were performed. Statistical analyses were performed using GraphPad Prism v7 (GraphPad Software Inc., San Diego, CA, USA), and *p*<0.05 was considered statistically significant.

RESULTS

Striatal gene expression changes in drug naïve *Per2* KO/WT mice

Microarray analyses indicated that 122 genes were differentially expressed in the striatum of drug naïve *Per2* KO/WT mice with |FC|≥2, *p*≤0.05 (Fig. 1). Among them, 64 genes were upregulated, and 58 genes were downregulated in *Per2* KO mice compared to WT mice (Supplementary Table 1, 2). Total DEGs, 122 genes in drug naïve *Per2* KO/WT mice were analyzed using GO analysis (Fig. 2). Results showed that DEGs in drug naïve groups were strongly enriched in response to channel activity, neurotransmitter receptor activity, G-protein coupled receptor (GPCR) activity, and serotonin receptor activity in molecular functions (Fig. 2A). These genes were also enriched in response to synaptic membrane, presynaptic membrane, integral component of synaptic membrane, intrinsic component of synaptic membrane, and dendritic membrane in cellular compartment (Fig. 2B). These results indicated that DEGs in *Per2* KO mice might be associated with synaptic structures and functions. All DEGs in drug naïve *Per2* KO/WT mice are also associated with membrane potential regulation, GPCR regulation, and responses to monoamine/catecholamine in biological process (Fig. 2C) indicating that DEGs in *Per2* KO would play important roles in GPCR-related neurotransmitter. In addition, KEGG analysis suggests that DEGs in drug naïve *Per2* KO/WT mice are also related with neuroactive ligand-receptor interaction, cAMP signaling, chemokine signaling, and cholinergic synapse pathways (Supplementary Fig. 1). These pathways are similar to the results of GO analysis results.

Striatal gene expression changes in drug naïve *Per2* KO/ *Per2* KO mice treated with METH

When the animals were treated with METH for 7 days, 90 genes were upregulated, and 347 genes were downregulated

A

Molecular function
Top 10 terms of GO functional analysis
adjusted *p* value<0.05 (*), 0.01 (**), 0.001 (***)

B

Cellular component
Top 9 terms of GO functional analysis
adjusted *p* value<0.05 (*), 0.01 (**), 0.001 (***)

C

Biological process
Top 6 terms of GO functional analysis
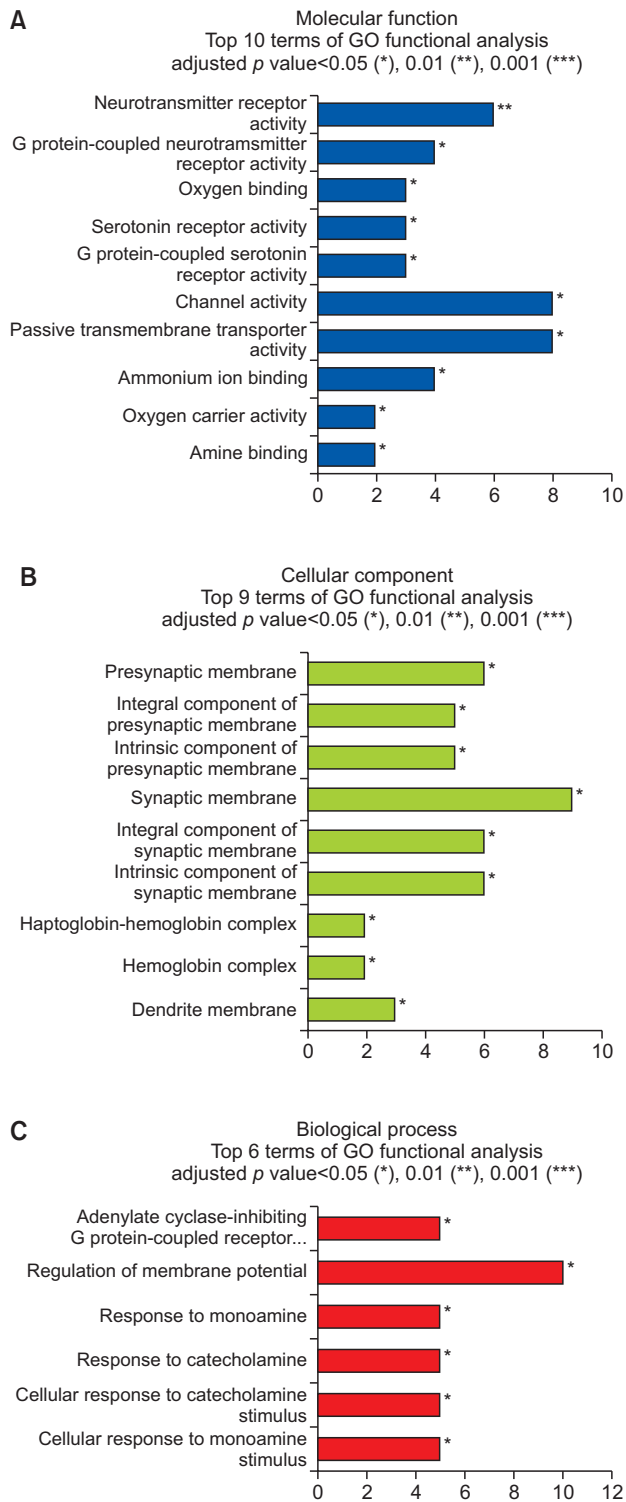adjusted *p* value<0.05 (*), 0.01 (**), 0.001 (***)

Fig. 2. Gene ontology (GO) enrichment analysis of DEGs between drug naïve *Per2* KO and WT mice. (A) Molecular process, (B) cellular component, and (C) biological process. *$p<0.05$, **$p<0.01$, ***$p<0.001$.

in *Per2* KO mice after treatment (Supplementary Table 3, 4). In GO analysis, 437 DEGs in *Per2* KO mice before and after METH treatment were strongly enriched in response to DNA-binding transcription activator activity, motor activity, and ATP-dependent microtubule motor activity in molecular functions (Fig. 3A). In the cellular compartment, the DEGs were strongly enriched in ciliary part, motile cilium, axoneme, and ciliary plasm (Fig. 3B). Additionally, 437 DEGs were also associated with membrane bound cell projection assembly, cell projection assembly, cilium organization, microtubule-based movement, and cilium movement in biological processes (Fig. 3C). These findings suggest that *Per2* roles in METH-induced responses might be associated with intracellular cilia or microtubule activities. In KEGG analysis, 437 DEGs were significantly enriched in neuroactive ligand-receptor interaction, cAMP signaling, PI3K-Akt signaling, actin cytoskeleton, and calcium signaling pathways (Supplementary Fig. 2). Results of the KEGG analysis in *Per2* KO before/after treatment with METH were similar to the results from drug naïve *Per2* KO/WT mice.

Selected DEGs in METH-induced dependent responses

We analyzed the common DEGs in drug naïve *Per2* KO/WT mice and before/after METH treatment in *Per2* KO mice to explore some of the potential genetic underpinnings of the relationship between *Per2* and METH-induced dependent responses. Firstly, we selected some DEGs associated with brain and drug addiction through literature searches. Among the total DEGs, 41 genes were chosen after literature searches in drug naïve *Per2* KO/WT mice, while 141 genes were chosen in *Per2* KO mice before and after METH treatment (Fig. 4). In WT mice before/after treatment with METH, only 23 genes were differentially expressed. We selected 9 genes that changed commonly in drug naïve *Per2* KO/WT mice and in *Per2* KO mice before/after METH treatment, but not in WT mice before/after METH. Interestingly, *Ncald*, *Cpa6*, *Pklr*, and *Ttc29* were upregulated in drug naïve *Per2* KO mice compared to drug naïve WT mice, while the genes were downregulated in *Per2* KO mice after METH treatment. *Cbr2*, *Egr2*, *Prg4*, *Lcn2*, and *Camsap2* were more downregulated in drug naïve *Per2* KO mice than in drug naïve WT mice, while the genes were more upregulated in *Per2* KO mice after METH treatment. qRT-PCR was used to confirm the selected 9 genes identified in microarray. All qRT-PCR results confirmed with the microarray results except *Ttc29* in *Per2* KO mice after METH treatment and *Camsap2* in drug naïve *Per2* KO mice (Fig. 5). In addition, GeneMANIA (http://www.genemania.org/) was used to predict the functions of the selected 9 genes (Fig. 6). Results of GeneMANIA suggested that the selected 8 genes except *Cbr2* might be associated with response to gonadotropin stimulus, response to cAMP, response to organophosphorus, and regulation of neuronal synaptic plasticity. To obtain the PPI network, the DEGs of the 9 target genes were entered into the STRING database. Fig. 7 shows the PPI network of target genes with 25 nodes and 20 edges (average node degree: 1.6, PPI enrichment *p* value: 7.15e-11).

DISCUSSION

The findings from our previous behavioral studies indicate that the dependence responses of chronic METH treatment are associated with the expression level of *Per2* as evidenced
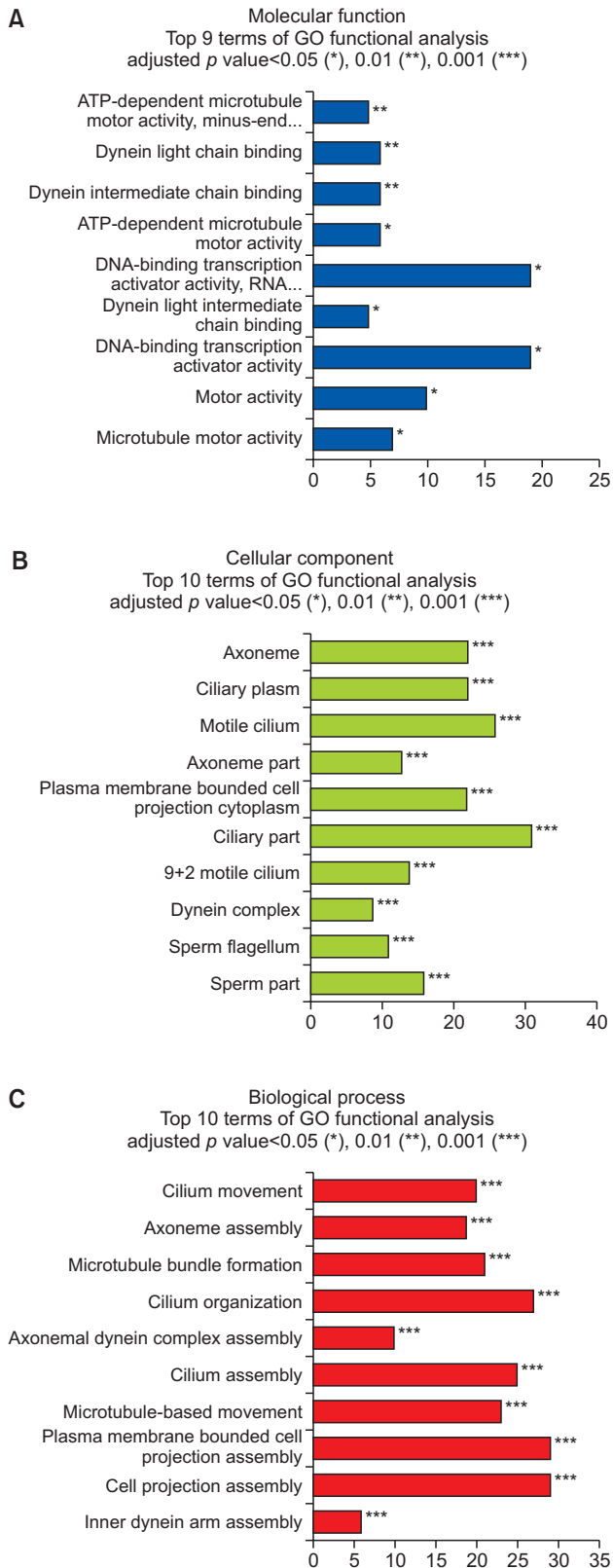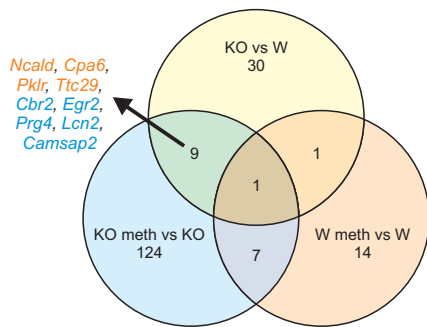
A

Molecular function
Top 9 terms of GO functional analysis
adjusted *p* value<0.05 (*), 0.01 (**), 0.001 (***)

B

Cellular component
Top 10 terms of GO functional analysis
adjusted *p* value<0.05 (*), 0.01 (**), 0.001 (***)

C

Biological process
Top 10 terms of GO functional analysis
adjusted *p* value<0.05 (*), 0.01 (**), 0.001 (***)

Fig. 3. Gene ontology (GO) enrichment analysis of DEGs in the *Per2* KO mice before and after METH treatment. (A) molecular process, (B) cellular component, and (C) biological process. *$p<0.05$, **$p<0.01$, ***$p<0.001$.

by more developed METH-induced locomotor sensitization and reward effects in *Per2* KO mice, while *Per2* overexpressed mice exhibited lesser responses against METH compared to WT mice (Kim *et al*., 2019). In addition to our previous study, increasing studies have reported that disrupted *Per2* expression can increase the vulnerability to drugs such as cocaine, alcohol, and morphine (Abarca *et al*., 2002; Spanagel *et al*., 2005; Perreau-Lenz *et al*., 2010; Brager *et al*., 2013). Several studies have attempted to reveal the mechanism of *Per2* in drug addiction, however it remains unclear. To elucidate the possible mechanisms of *Per2* in METH-induced dependence responses, we analyzed DEGs in the striatum of *Per2* KO and WT mice before and after METH treatment. Disruption of *Per2* might regulate alterations in the expression of multiple genes that are associated with biological functions.

Among the common DEGs in drug naïve *Per2* KO/WT mice and before/after METH treatment in *Per2* KO mice, *Cpa6* is the gene encoding Carboxypeptidase A6 (CPA6), a metallo-carboxypeptidase enzyme. CPA6 converts enkephalins and neurotensin into inactive forms (Lyons *et al*., 2008). Neurotensin is an endogenous neuropeptide known to modulate dopaminergic pathways (Kasckow and Nemeroff, 1991; Binder *et al*., 2001). Enhanced neurotensin decreased dopamine release in the NAc and blocked stimulant-induced hyper-locomotor activity (Binder *et al*., 2001; Servonnet *et al*., 2017). Previous studies using *Per2* transgenic (TG) mice have reported that disruption or overexpression of *Per2* might lead to changes in dopaminergic systems and stimulant-induced behavior responses (Abarca *et al*., 2002; Hampp *et al*., 2008; Kim *et al*., 2018, 2019). In contrast, alteration of the dopamine expression level influenced *Per2* expression (Hood *et al*., 2010; Gravotta *et al*., 2011). All these results suggest that *Per2* may influence stimulant-induced dependence responses through the interaction of *Cpa6*, neurotensin, and dopamine. However, PPI networks (Fig. 7) did not exhibit any network between *Cpa6* and neurotensin-related proteins, although some studies have reported the relationship between them. Thus, further studies are required to deepen our insights into the relationship between *Per2* and *Cpa6* on drug dependence.

Egr2 (also termed *Krox20*) belongs to the family of early growth response (Egr) genes associated with neuronal development (Gabet *et al*., 2010; dela Peña *et al*., 2015). *Egr2* is also associated with long-term potentiation (Williams *et al*., 1995; Belluardo *et al*., 2005). Belluardo and colleagues (2005) reported that *Egr2* may play key roles as a cognitive enhancer in nicotine dependence (Belluardo *et al*., 2005). Growing studies have reported the changes of *Egr2* expression by drug administration. Rats treated with heroin demonstrated an increase in *Egr2* expression and exhibited reinforcement effects and conditioned place preference (CPP) against heroin (Kuntz *et al*., 2008; Xia *et al*., 2018). Chronic morphine treatment increased *Krox20* (*Egr2*), *Per2*, and cAMP responsive element binding protein (CREB) in the frontal cortex of Wistar rats (Ammon *et al*., 2003). The spontaneously hypertensive rat (SHR) treated with amphetamine also showed increased expression level of *Egr2* and *Per2* in the striatum and exhibited reinforcement effects and CPP (dela Peña *et al*., 2015). METH administration induced changes in *Egr2* expression in the striatum. Acute METH treatment increased *Egr2* expression in the striatum of rats, while chronic METH administration decreased *Egr2* and *Creb* expressions (McCoy *et al*., 2011). Based on these results, we can assume that *Per2* may influence drug

A

Ncald, Cpa6, Pklr, Ttc29, Cbr2, Egr2, Prg4, Lcn2, Camsap2

KO vs W 30

KO meth vs KO 124

W meth vs W 14

9

1

1

7

B

Gene symbol	Gene title	Fc in drug naïve *Per2* KO/WT	Fc in before/ after METH in *Per2* KO
Ncald	Neurocalcin delta	4.51	−4.92
Cpa6	Carboxypeptidase A6	3.52	−3.82
Pklr	Pyruvate kinase liver and red blood cell	3.02	−4.63
Ttc29	Tetratricopeptide repeat domain 29	2.26	−3.51
Lcn2	Lipocalin 2	−34.51	56.14
Prg4	Proteoglycan 4 (megakaryocyte stimulating factor, articular superficial zone protein)	−6.09	7.19
Camsap2	Calmodulin regulated spectrin-associated protein family, member2	−3.33	3.21
Egr2	Early growth response 2	−2.3	6.45
Cbr2	Carbonyl reductase 2	−2.2	2.18

Fig. 4. Venn diagrams and target genes. (A) Venn diagrams showing the number of DEGs in the striatum of drug naïve *Per2* KO/WT mice, before/after METH in *Per2* KO mice, and before/after METH in WT mice (B) target genes that commonly changed in drug naïve *Per2* KO/ WT mice, and before/after METH in *Per2* KO mice that showed more vulnerable responses against METH.

addiction through *Egr2* and *Creb* activities. Our PPI networks also show the relationship between EGR2 and CREB (Fig. 7).

LCN2 is an iron-related protein encoded by lipocalin 2 (*Lcn2*) that enhances the activation of nuclear factor kappa B subunit 2 (NF-κB) pathway (Ye *et al*., 2014). LCN2 also establishes a network with *Egr2* through NF-κB in our PPI networks. Some previous studies have reported that NF-κB plays key roles in drug rewarding effects and drug-related memory (Zhang *et al*., 2011; Ferreira *et al*., 2013). Inhibition of NF-κB blocked CPP against morphine. In contrast to these studies, *Lcn2* expression reduced after chronic morphine treatment (Ye *et al*., 2014). *Lcn2* also participates in the regulation of spine morphology and neuronal excitability (Mucha *et al*., 2011; Ferreira *et al*., 2013). Upregulated *Lcn2* induced a reduction in dendritic spine actin's mobility in the hippocampus of mice (Mucha *et al*., 2011). Recently, several studies have suggested that increased *Lcn2* expression might be associated with neurotoxicity and neuroinflammation of dopamine neurons (Kim *et al*., 2016; Xu *et al*., 2018). In contrast, LCN2 null mice exhibited decreased LTP in the hippocampus and impaired cognitive abilities in special learning tests (Ferreira *et al*., 2013). Although some studies reviewed various functions of *Lcn2* in the central nervous system (Ferreira *et al*., 2015; Jha *et al*., 2015), evidences to support the roles of *Lcn2* in drug addiction are not sufficient. Thus, further studies are required to confirm the relationship between *Per2* and *Lcn2* in drug addiction.

It was also reported that neurocalcin delta (*Ncald*), a member of the neuronal calcium sensor (NCS) family, was associated with neuronal morphology. Overexpressed *Ncald* induced a reduction in axon outgrowth and branching of cultured hippocampal neurons (Yamatani *et al*., 2010), and *Ncald* KO restored axonal growth in zebrafish and mice (Riessland *et al*., 2017). In contrast, Upadhyay *et al*. (2019) reported that *Ncald* KO impaired neurogenesis in adult mice, while *Ncald* heterozygous mice did not exhibit significant changes. Additionally, *Ncald* was downregulated in the obesity-induced memory impairment animal model (Ma *et al*., 2017). Thus, the study suggested that *Ncald* might play important roles in memory. Consistently, *Ncald* expression was lower in patients with Alzheimer's disease (Shimohama *et al*., 1996; Miller *et*

al., 2013). *Ncald* is also associated with coffee and caffeine consumption (Yamamoto *et al*., 2015; Lee, 2018). *Ncald* is one of the SNPs associated with coffee consumption. However, evidences showing the relationship between *Ncald* and substance dependence are insufficient. In addition, NCALD encoded by *Ncald* is one of the key proteins that contribute to the release of neurotransmitters (Ivings *et al*., 2002; Vercauteren *et al*., 2007). Thus, *Ncald* might be a good target to better understand drug addiction.

PRG4 (proteoglycan4), also known as lubricin, encoded by *Prg4*, acts as a joint lubricant. Interestingly, *Prg4* expression significantly changed in the striatum of drug naïve *Per2* KO and WT mice, and before and after METH treatment in *Per2* KO mice, but not before and after METH treatment in WT mice. Some previous studies reported that *Prg4* expression was associated with cAMP activities in chondrocyte or synoviocyte (Wu *et al*., 2017; Qadri *et al*., 2018). Wu *et al*. (2017) reported that the kappa opioid receptor agonist induced changes of *Prg4* expression through the cAMP/CREB pathway. Taken together, *Prg4* could be one of the new candidates to elucidate the drug addiction pathway.

We found that the roles of selected common DEGs reported by other previous studies are associated with the GO and KEGG analyses of total DEGs such as intrinsic component of synaptic membrane, dendritic membrane in cellular components, calcium signaling pathways, GPCR regulation, cAMP signaling, etc., which have relevance to drug addiction pathways. This fact indicates that the selected common DEGs including *Cpa6*, *Ncald*, *Egr2*, *Lcn2*, and *Prg4*, might play key roles in drug addiction, and their pathways may be associated with *Per2* regulation. *Per2* KO mice exhibited more vulnerable METH addiction responses in our previous study, and in the current study, we found the expression levels of some genes such as *Cpa6*, *Ncald*, *Egr2*, *Lcn2*, and *Prg4* changed in *Per2* KO mice after METH treatments. Taken together, the selected genes might play key roles in vulnerable responses of *Per2* KO mice against METH. Furthermore, the potential pathway of the selected 5 genes (*Cpa6*, *Ncald*, *Egr2*, *Lcn2*, and *Prg4*) under *Per2* regulation is illustrated in Fig. 8. Thus, further studies should be performed to investigate the link between these genes and the effects on drug dependence responses. These
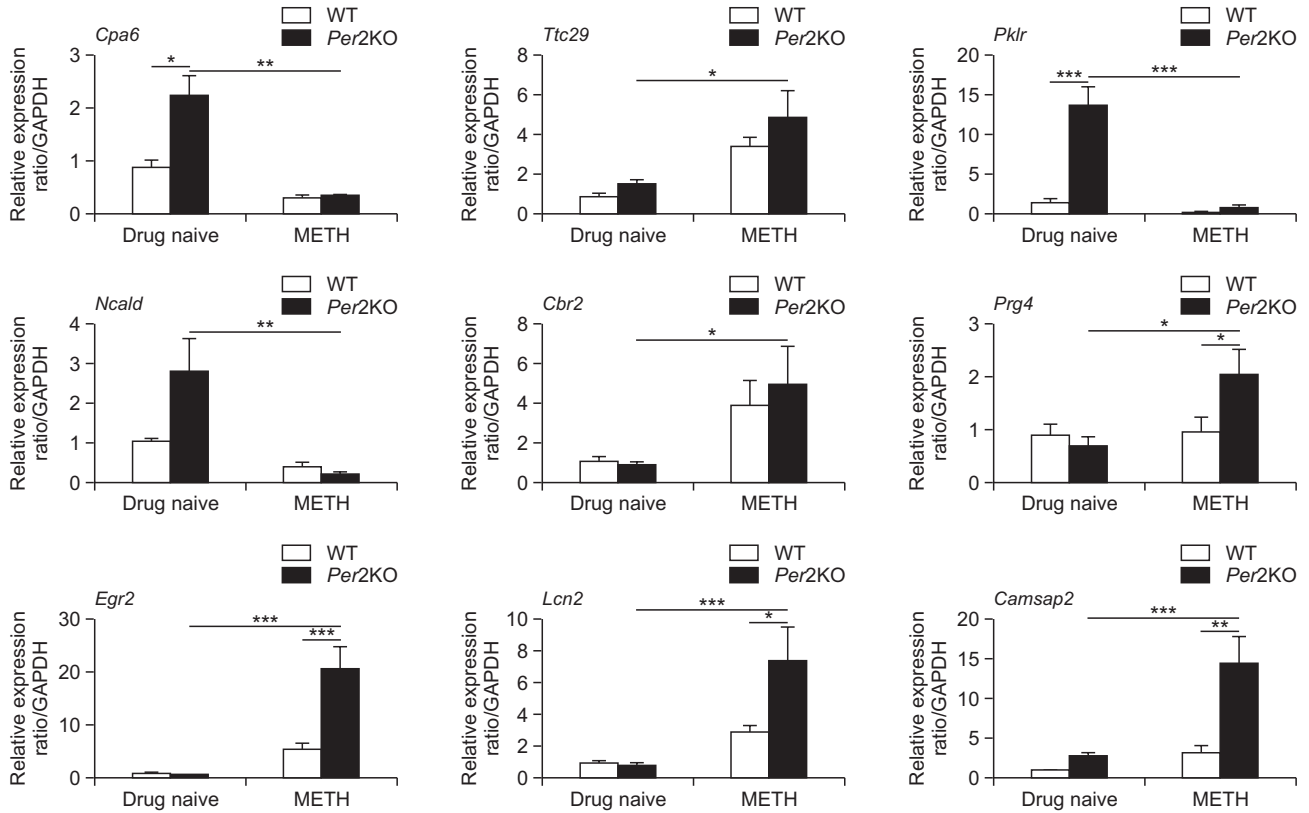
Fig. 5. Confirmed changes in the striatal gene expression of *Per2* KO and WT mice. qRT-PCR validated expressions of target genes (*Ncald*, *Cpa6*, *Pklr*, *Ttc29*, *Cbr2*, *Egr2*, *Prg4*, *Lcn2*, and *Camsap2*) in the striatum of *Per2* KO and WT mice before and after METH chronic treatments. *$p < 0.05$, **$p < 0.01$, ***$p < 0.001$.
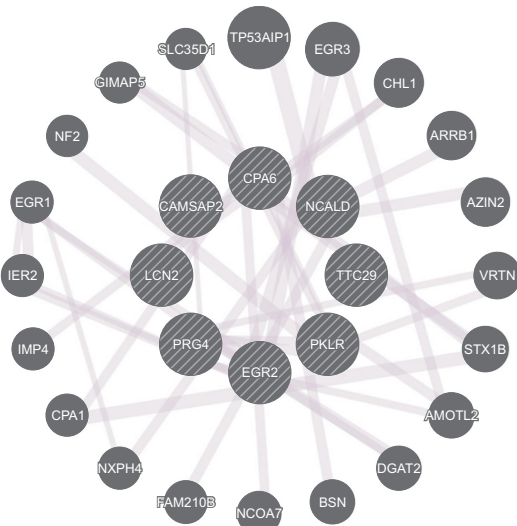

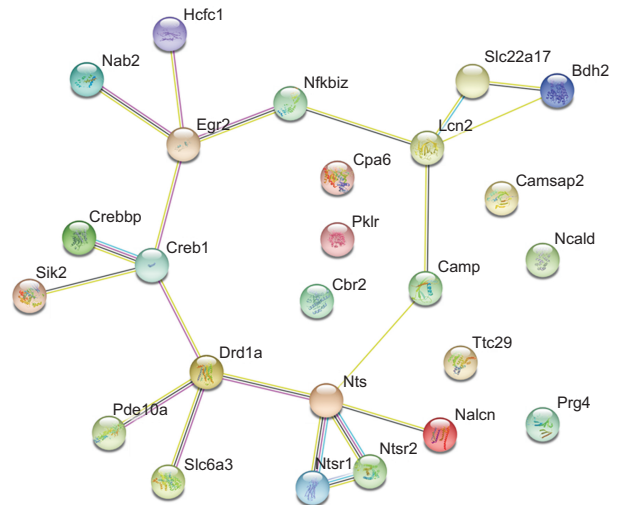**Fig. 6.** Network analysis of target genes by GeneMANIA.

Fig. 7. Network analysis of target genes by STRING. Results of protein-protein interaction (PPI) network for the target genes from STRING database. PPI network of target genes shows 25 nodes and 20 edges (average node degree: 1.6, PPI enrichment p value: 7.15e-11).
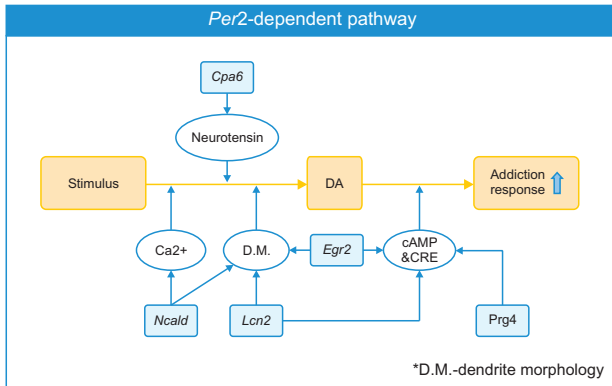
Fig. 8. Schematic diagram (*Per2*-mediated addiction behavior hypothesis). Diagram illustrates that *Per2* expression might influence drug addiction through the pathways of target genes.

target genes would be new candidates to reveal the mechanisms of drug addiction.

CONFLICT OF INTEREST

The authors declare that they have no conflicts of interest.

ACKNOWLEDGMENTS

REFERENCES

Abarca, C., Albrecht, U. and Spanagel, R. J. (2002) Cocaine sensitization and reward are under the influence of circadian genes and rhythm. *Proc. Natl. Acad. Sci. U.S.A.* **99**, 9026-9030.

Albrecht, U., Zheng, B., Larkin, D., Sun, Z. S. and Lee, C. C. (2001) mPer1 and mPer2 are essential for normal resetting of the circadian clock. *J. Biol. Rhythms* **16**, 100-104.

Ammon, S., Mayer, P., Riechert, U., Tischmeyer, H. and Höllt, V. J. (2003) Microarray analysis of genes expressed in the frontal cortex of rats chronically treated with morphine and after naloxone precipitated withdrawal. *Mol. Brain Res.* **112**, 113-125.

Bae, K., Jin, X., Maywood, E. S., Hastings, M. H., Reppert, S. M. and Weaver, D. R. (2001) Differential functions of mPer1, mPer2, and mPer3 in the SCN circadian clock. *Neuron* **30**, 525-536.

Belluardo, N., Olsson, P., Mudo, G., Sommer, W., Amato, G. and Fuxe, K. (2005) Transcription factor gene expression profiling after acute intermittent nicotine treatment in the rat cerebral cortex. *Neuroscience* **133**, 787-796.

Binder, E. B., Kinkead, B., Owens, M. J. and Nemeroff, C. B. (2001) Neurotensin and dopamine interactions. *Pharmacol. Rev.* **53**, 453-486.

Brager, A. J., Stowie, A. C., Prosser, R. A. and Glass, J. D. (2013) The mPer2 clock gene modulates cocaine actions in the mouse circadian system. *Behav. Brain Res.* **243**, 255-260.

Caprioli, D., Venniro, M., Zhang, M., Bossert, J. M., Warren, B. L., Hope, B. T. and Shaham, Y. (2017) Role of dorsomedial striatum neuronal ensembles in incubation of methamphetamine craving after voluntary abstinence. *J. Neurosci.* **37**, 1014-1027.

Chang, L., Alicata, D., Ernst, T. and Volkow, N. (2007) Structural and metabolic brain changes in the striatum assoicated with methamphetamine abuse. *Addiction* **102**, 16-32.

dela Peña, I., de la Peña, J. B., Kim, B. N., Han, D. H., Noh, M. and Cheong, J. H. (2015) Gene expression profiling in the striatum of amphetamine-treated spontaneously hypertensive rats which showed amphetamine conditioned place preference and self-administration. *Arch. Pharm. Res.* **38**, 865-875.

Everitt, B. J. and Robbins, T. W. (2016) Drug addiction: updating actions to habits to compulsions ten years on. *Annu. Rev. Psychol.* **67**, 23-50.

Ferreira, A. C., Da Mesquita, S., Sousa, J. C., Correia-Neves, M., Sousa, N., Palha, J. A. and Marques, F. (2015) From the periphery to the brain: Lipocalin-2, a friend or foe? *Prog. Neurobiol.* **131**, 120-136.

Ferreira, A. C., Pinto, V., Mesquita, S. D., Novais, A., Sousa, J. C., Correia-Neves, M., Sousa, N., Palha, J. A. and Marques, F. (2013) Lipocalin-2 is involved in emotional behaviors and cognitive function. *Front. Cell. Neurosci.* **7**, 122.

Gabet, Y., Baniwal, S. K., Leclerc, N., Shi, Y., Kohn-Gabet, A. E., Cogan, J., Dixon, A., Bachar, M., Guo, L., Turman, J. E., Jr. and Frenkel, B. (2010) Krox20/EGR2 deficiency accelerates cell growth and differentiation in the monocytic lineage and decreases bone mass. *Am. J. Hematol.* **116**, 3964-3971.

Gravotta, L., Gavrila, A. M., Hood, S. and Amir, S. J. (2011) Global depletion of dopamine using intracerebroventricular 6-hydroxydopamine injection disrupts normal circadian wheel-running patterns and PERIOD2 expression in the rat forebrain. *J. Mol. Neurosci.* **45**, 162-171.

Hampp, G., Ripperger, J. A., Houben, T., Schmutz, I., Blex, C., Perreau-Lenz, S., Brunk, I., Spanagel, R., Ahnert-Hilger, G., Meijer, J. H. and Albrecht, U. (2008) Regulation of monoamine oxidase A by circadian-clock components implies clock influence on mood. *Curr. Biol.* **18**, 678-683.

Hasler, B., Smith, L., Cousins, J. and Bootzin, R. J. (2012) Circadian rhythms, sleep, and substance abuse. *Sleep Med. Rev.* **16**, 67-81.

Hood, S., Cassidy, P., Cossette, M. P., Weigl, Y., Verwey, M., Robinson, B., Stewart, J. and Amir, S. (2010) Endogenous dopamine regulates the rhythm of expression of the clock protein PER2 in the rat dorsal striatum via daily activation of D2 dopamine receptors. *J. Neurosci.* **30**, 14046-14058.

Ivings, L., Pennington, S. R., Jenkins, R., Weiss, J. L. and Burgoyne, R. D. (2002) Identification of Ca2+-dependent binding partners for the neuronal calcium sensor protein neurocalcin δ: interaction with actin, clathrin and tubulin. *Biochem. J.* **363**, 599-608.

Jha, M. K., Lee, S., Park, D. H., Kook, H., Park, K. G., Lee, I. K. and Suk, K. (2015) Diverse functional roles of lipocalin-2 in the central nervous system. *Neurosci. Biobehav. Rev.* **49**, 135-156.

Kasckow, J. and Nemeroff, C. B. (1991) The neurobiology of neurotensin: focus on neurotensin-dopamine interactions. *Regul. Pept.* **36**, 153-164.

Kim, B. W., Jeong, K. H., Kim, J. H., Jin, M., Kim, J. H., Lee, M. G., Choi, D. K., Won, S. Y., McLean, C., Jeon, M. T., Lee, H. W., Kim, S. R. and Suk, K. (2016) Pathogenic upregulation of glial lipocalin-2 in the parkinsonian dopaminergic system. *J. Neurosci.* **36**, 5608-5622.

Kim, M., Custodio, R. J., Botanas, C. J., de la Peña, J. B., Sayson, L. V., Abiero, A., Ryoo, Z. Y., Cheong, J. H. and Kim, H. J. (2019) The circadian gene, Per2, influences methamphetamine sensitization and reward through the dopaminergic system in the striatum of mice. *Addict. Biol.* **24**, 946-957.

Kim, M., De La Pena, J. B., Cheong, J. H. and Kim, H. J. J. (2018) Neurobiological functions of the period circadian clock 2 gene, Per2. *Biomol. Ther. (Seoul)* **26**, 358-367.

Kovanen, L., Saarikoski, S. T., Haukka, J., Pirkola, S., Aromaa, A., Lönnqvist, J. and Partonen, T. (2010) Circadian clock gene polymorphisms in alcohol use disorders and alcohol consumption. *Alcohol Alcohol.* **45**, 303-311.

Kuntz, K. L., Patel, K. M., Grigson, P. S., Freeman, W. M. and Vrana, K. E. (2008) Heroin self-administration: II. CNS gene expression following withdrawal and cue-induced drug-seeking behavior. *Pharmacol. Biochem. Behav.* **90**, 349-356.

Lee, Y. H. (2018) Investigating the possible causal association of cof-

fee consumption with osteoarthritis risk using a Mendelian random-ization analysis. *Clin. Rheumatol.* **37**, 3133-3139.

Lyons, P. J., Callaway, M. B. and Fricker, L. D. (2008) Characterization of carboxypeptidase A6, an extracellular matrix peptidase. *J. Biol. Chem.* **283**, 7054-7063.

Ma, W. W., Ding, B. J., Yuan, L. H., Zhao, L., Yu, H. L. and Xiao, R. (2017) Neurocalcin-delta: a potential memory-related factor in hip-pocampus of obese rats induced by high-fat diet. *Afr. Health Sci.* **17**, 1211-1221.

McCoy, M. T., Jayanthi, S., Wulu, J. A., Beauvais, G., Ladenheim, B., Martin, T. A., Krasnova, I. N., Hodges, A. B. and Cadet, J. L. (2011) Chronic methamphetamine exposure suppresses the striatal ex-pression of members of multiple families of immediate early genes (IEGs) in the rat: normalization by an acute methamphetamine in-jection. *Psychopharmacology (Berl.)* **215**, 353-365.

Miller, J. A., Woltjer, R. L., Goodenbour, J. M., Horvath, S. and Ge-schwind, D. H. (2013) Genes and pathways underlying regional and cell type changes in Alzheimer's disease. *Genome Med.* **5**, 48.

Mucha, M., Skrzypiec, A. E., Schiavon, E., Attwood, B. K., Kucerova, E. and Pawlak, R. (2011) Lipocalin-2 controls neuronal excitability and anxiety by regulating dendritic spine formation and matura-tion. *Proc. Natl. Acad. Sci. U.S.A.* **108**, 18436-18441.

Nestler, E. J. and Malenka, R. C. (2004) The addicted brain. *Sci. Am.* **290**, 78-85.

Perreau-Lenz, S., Sanchis-Segura, C., Leonardi-Essmann, F., Schnei-der, M. and Spanagel, R. (2010) Development of morphine-in-duced tolerance and withdrawal: involvement of the clock gene mPer2. *Eur. Neuropsychopharmacol.* **20**, 509-517.

Qadri, M. M., Jay, G. D., Ostrom, R. S., Zhang, L. X. and Elsaid, K. A. (2018) cAMP attenuates TGF-β's profibrotic responses in osteoar-thritic synoviocytes: involvement of hyaluronan and PRG4. *Am. J. Physiol. Cell Physiol.* **315**, C432-C443.

Riessland, M., Kaczmarek, A., Schneider, S., Swoboda, K. J., Löhr, H., Bradler, C., Grysko, V., Dimitriadi, M., Hosseinibarkooie, S., Torres-Benito, L., Peters, M., Upadhyay, A., Biglari, N., Kröber, S., Hölker, I., Garbes, L., Gilissen, C., Hoischen, A., Nürnberg, G., Nürnberg, P., Walter, M., Rigo, F., Bennett, C. F., Kye, M. J., Hart, A. C., Ham-merschmidt, M., Kloppenburg, P. and Wirth, B. (2017) Neurocalcin delta suppression protects against spinal muscular atrophy in hu-mans and across species by restoring impaired endocytosis. *Am. J. Hum. Genet.* **100**, 297-315.

Servonnet, A., Minogianis, E. A., Bouchard, C., Bédard, A. M., Lévesque, D., Rompré, P. P. Samaha, A. N. (2017) Neurotensin in the nucleus accumbens reverses dopamine supersensitivity evoked by antipsychotic treatment. *Neuropharmacology* **123**, 10-21.

Shimohama, S., Chachin, M., Taniguchi, T., Hidaka, H. and Kimura, J. (1996) Changes of neurocalcin, a calcium-binding protein, in the brain of patients with Alzheimer's disease. *Brain Res.* **716**, 233-236.

Solinas, M., Belujon, P., Fernagut, P. O., Jaber, M. and Thiriet, N. J.

(2019) Dopamine and addiction: what have we learned from 40 years of research. *J. Neural Transm. (Vienna)* **126**, 481-516.

Spanagel, R., Pendyala, G., Abarca, C., Zghoul, T., Sanchis-Segura, C., Magnone, M. C.,Lascorz, J., Depner, M., Holzberg, D., Soyka, M., Schreiber, S., Matsuda, F., Lathrop, M., Schumann, G. and Al-brecht, U. (2005) The clock gene Per2 influences the glutamatergic system and modulates alcohol consumption. *Nat. Med.* **11**, 35-42.

Upadhyay, A., Hosseinibarkooie, S., Schneider, S., Kaczmarek, A., Torres-Benito, L., Mendoza-Ferreira, N., Overhoff, M., Rombo, R., Grysko, V., Kye, M. J., Kononenko, N. L. and Wirth, B. (2019) Neu-rocalcin delta knockout impairs adult neurogenesis whereas half reduction is not pathological. *Front. Mol. Neurosci.* **12**, 19.

Vercauteren, F. G., Flores, G., Ma, W., Chabot, J. G., Geenen, L., Clerens, S., Fazel, A., Bergeron, J. J., Srivastava, L. K., Arckens, L. and Quirion, R. (2007) An organelle proteomic method to study neurotransmission-related proteins, applied to a neurodevelop-mental model of schizophrenia. *Proteomics* **7**, 3569-3579.

Volkow, N. D., Wise, R. A. and Baler, R. J. (2017) The dopamine mo-tive system: implications for drug and food addiction. *Nat. Rev. Neurosci.* **18**, 741-752.

Williams, J., Dragunow, M., Lawlor, P., Mason, S., Abraham, W., Leah, J., Bravo,R., Demmer, J. and Tate, W. (1995) Krox20 may play a key role in the stabilization of long-term potentiation. *Mol. Brain Res.* **28**, 87-93.

Wu, L., Zhang, S., Shkhyan, R., Lee, S., Gullo, F., Eliasberg, C. D., Petrigliano, F. A., Ba, K., Wang, J., Lin, Y. J. and Evseenko, D. (2017) Kappa opioid receptor signaling protects cartilage tissue against posttraumatic degeneration. *JCI Insight* **2**, e88553.

Xia, B., Li, Y., Li, R., Yin, D., Chen, X., Li, J. and Liang, W. (2018) Ef-fect of sirtuin-1 on synaptic plasticity in nucleus accumbens in a rat model of heroin addiction. *Med. Sci. Monit.* **24**, 3789-3803.

Xu, H., Wang, Y., Song, N., Wang, J., Jiang, H. and Xie, J. (2018) New progress on the role of glia in iron metabolism and iron-induced degeneration of dopamine neurons in Parkinson's disease. *Front. Mol. Neurosci.* **10**, 455.

Yamamoto, V. J., Paula, V. d. J. R. d., Forlenza, O. V., Santos, B. D. and Kerr, D. S. (2015) Association study in Alzheimer's disease of single nucleotide polymorphisms implicated with coffee consump-tion. *Arch. Clin.* **42**, 69-73.

Yamatani, H., Kawasaki, T., Mita, S., Inagaki, N. and Hirata, T. (2010) Proteomics analysis of the temporal changes in axonal proteins during maturation. *Dev. Neurobiol.* **70**, 523-537.

Ye, J., Yang, Z., Li, C., Cai, M., Zhou, D., Zhang, Q., Wei, Y., Wang, T. and Liu, Y. (2014) NF-κB signaling and vesicle transport are cor-related with the reactivation of the memory trace of morphine de-pendence. *Diagn. Pathol.* **9**, 142.

Zhang, X., Cui, Y., Jing, J., Cui, Y., Xin, W. and Liu, X. (2011) Involve-ment of p38/NF-κB signaling pathway in the nucleus accumbens in the rewarding effects of morphine in rats. *Behav. Brain Res.* **218**, 184-189.